

Concrete Shielding Thickness Requirements for PET Facilities

V. Steiner¹, A. Malki¹, T. Ben-Yehuda¹, M. Moinester^{2*}

¹Department of Nuclear Medicine, Sheba Medical Center, 5262000 Ramat Gan, Israel

²School of Physics and Astronomy, Tel Aviv University, 69978 Tel Aviv, Israel

*Corresponding author's email: murraym@tauphy.tau.ac.il

ABSTRACT

This study aims to determine the protective concrete shielding thickness requirements in concrete walls of positron emission tomography (PET) and computed tomography (CT) facilities. Consider the most commonly used PET radiotracer, the radioisotope F^{18} , which emits two back-to-back 511 keV photons. Photon transmission measurements were carried out through an Israeli B30 strength ordinary concrete wall (3 meter high, 20 cm thick) using photons emitted from an F^{18} source into a cone having a 24 degree FWHM dose aperture angle. The source, positioned 3 meters from the wall, yielded a 0.64 m beam disk radius on the wall. Our measurement setup roughly simulates radiation emitted from a patient injected with F^{18} . Dose rates were measured by an Atomtex AT1123 Radiation Survey Meter, positioned at distances 0.05 to 3 meters from the far side of the wall. For a wide-beam, thick-shielding setup, there is a “buildup” effect, as photons having reduced energies may reach the detector from Compton scattering in the wall. In concrete, the Compton scattering cross section accounts for 99% of the total interaction cross section. The buildup factor B accounts for the increase of observed radiation transmission through shielding material due to scattered radiation. We measured a narrow-beam transmission coefficient $T=3.0 \pm 0.9 \%$, consistent with the theoretical value 2% calculated from NIST photon attenuation data without buildup. We measured a wide-beam transmission coefficient of $8.6 \pm 1.8\%$; in good agreement with two available wide-beam Monte Carlo (MC) simulations. We confirm by experiment, complementing MC simulations, that for a 20 cm thick concrete wall, due to buildup, about four times thicker shielding is required to achieve a designated level of radiation protection, compared to that calculated using narrow-beam, thin-shielding transmission coefficients.

Keywords: photons, FDG, PET, CT, concrete, lead, radiation shielding, buildup factors

1 Introduction

This study deals with protective concrete shielding walls of positron emission tomography (PET) and computed tomography (CT) facilities, similar to those at the Sheba Hospital (Israel) [1]. PET aided diagnosis is based on radioisotope imaging following administration of a radioactive isotope. The images show how the radioactive isotope binds to the selected target tissues. The most commonly used PET radiotracer is the radioisotope F^{18} . It has a 1.8 hour physical half-life, and a 1.4 hour effective life time (physical and biological). In its dominant decay mode (97%), it emits a positron having 250 keV mean energy. After the positron stops in about 1.2 mm of tissue, it annihilates with an electron, and two 511 keV gamma rays (photons) are emitted isotopically back-to-back. After 4 hours, the patient's F^{18} radioactivity falls to about 14% of the typical 10 mCi internal activity injected for PET scans. Shielding walls in PET facilities are used to provide low cost shielding to protect hospital staff from a patient's radiation during the entire time that the patient remains in the hospital. Wall photon transmission measurements were carried out to determine the thickness of concrete required to satisfy radiation protection safety regulations. The transmission coefficient T of photons traversing shielding material having density ρ (g/cm³), mean atomic number Z , linear attenuation coefficient μ (in cm⁻¹), mass attenuation coefficient $\mu_m = \mu/\rho$ (cm²/g), shielding thickness x (cm), buildup coefficient $B(E,Z,x)$, incident photon intensity I_0 , transmitted photon intensity I , and a photon energy E , may be expressed as [2]:

$$T=I/I_0 = B(E, Z, x) \exp(-\mu x) \quad (1)$$

When a narrow photon beam traverses material, only photons traveling directly along the beam axis, without scattering, reach a downstream small-size detector positioned on the beam axis. When a wide photon beam of the same photon intensity traverses material, photons may scatter into the direction of the detector, increasing the detected radiation with respect to the narrow beam geometry. The buildup factor B accounts for the increase of observed radiation transmission through shielding material due to scattered radiation. For a given material, B depends on E , Z , x , μ and beam geometry (narrow, wide, or conically emitted from a localized source). For a narrow beam and thin shielding, $B=1$. For a wide beam and thick shielding, the average photon energy reaching the detector is less than 511 keV, as lower energy photons may reach the dose detector following Compton scattering in the wall. As a result, the buildup coefficient B can become large, and the transmission coefficient would increase above the narrow-beam, thin-shielding value. Thick shielding would then be needed to provide sufficient radiation protection, rather than the thin thickness calculated using $B=1$ tabulated narrow-beam transmission coefficients.

For 511 keV photon energies, typical of PET radiotracers, depending on the mean atomic number of the shielding wall, attenuation proceeds via photoelectric absorption and/or Compton scattering. In photoelectric absorption, the photon is removed completely through the transfer of all its energy to an electron in the shielding material. In Compton scattering, a photon transfers part of its energy to an electron in the shielding material. The scattered photon may then undergo additional Compton scattering or photoelectric absorption interactions, and may finally exit the shielding material with reduced energy [2].

The buildup factor B is usually estimated by Monte Carlo (MC) simulation calculations, and tabulated according to Z , E , μ and shielding thickness measured in units of $\lambda = 1/\mu$ mean free paths (mfp). For ordinary concrete having $\rho=2.35$ g/cm³, $\lambda=5.1$ cm, the appropriate MC table shielding thickness value is ~ 4 mfp. The value $\mu_m = 0.0833$ cm²/g ($\mu=0.196$ cm⁻¹) given by Stankovic et al [3] is taken for all calculations. It is close to the NIST value at 500 keV of 0.0877 cm²/g [4].

2 Research Methodology

F¹⁸ Source

The measurements employed photons emitted from a liquid Fludeoxyglucose (FDG) F¹⁸ source [6]. A schematic drawing of the source assembly is shown in Fig.1. The source activity was 23.4 mCi (865 MBq) at the start of measurements. Since F¹⁸ decays mainly by emitting two 511 keV photons back-to-back, one therefore expects 8.65×10^8 emitted photons per second into the forward hemisphere. The FDG was held in a 20 ml glass vial in a saline (NaCl) solution having density ~ 1 g/cm³. The vial was secured inside a 2 cm thick tungsten container, inside a 1 cm thick lead-plated transportation box. The thick tungsten walls allowed photons to exit only through a geometric opening angle of 32°, through a thin 0.3 cm thick cylindrical tungsten collimator, having diameter 2 cm and a central 1 cm diameter aperture. Aside from a small component of back scattering, forward emitted photons exit the source either through the collimator's aperture or by transmission through its 0.3 cm thickness. The central aperture is expected to transmit mainly the non-interacting 511 keV photons emitted from about 20% of the source volume. The rest are absorbed in the tungsten container. The overall transmission coefficient out of the transportation box was 0.1%, ensuring a low radiation field at 1 m distance from the box. Only about 80% of the vial was filled. This feature lowered the emission probability of the source when rotated 90° for measurement in the horizontal direction, since the volume of an imaginary cylinder in the middle of the vial with 2 cm diameter equal to that of the collimator was not completely filled with liquid. Only photons emitted from source liquid within this cylinder are geometrically positioned to efficiently exit through the collimator.

At 511 keV, the photon interaction cross sections with tungsten, for coherent (Rayleigh), incoherent (Compton) and photoelectric effects are 2.9, 21.0 and 18.2 barn, respectively. The total cross section is 42.1 barn. The relative interaction probabilities are 7%, 50%, 43%. In coherent scattering, the angular distribution is isotropic and the energy does not change with scattering angle. In Compton interactions, scattered photons have energies between 170 and 511 keV; the larger the scattering angle, the lower the energy. The angular distribution is forward peaked, with 75% of the photons emitted in the forward hemisphere, based on the Compton (Klein-Nishima) photon angular distribution at 511 keV. In photoelectric events, the photons are absorbed.

The mean free path (mfp) of photoelectric absorption in tungsten at 511 keV is 0.32 cm. This is relevant since photons are stopped efficiently in the collimator only by the photoelectric effect. As a result, the 0.3 cm thick tungsten collimator sheet should transmit about 40% of the incident direct (511 keV) photons. Part of them will exit with reduced energy because of Compton scattering. The mfp for photoelectric absorption in tungsten between 511 keV and 170 keV decreases sharply with decreasing energy. At 300 keV it is 0.09 cm leading to only 3% transmission. Photon exiting the source through the collimator are therefore expected to have between 511 and 300 keV, strongly peaked at 511 keV.

Based on source geometry, roughly 30% of the 8.65×10^8 photons per second forward emitted by F^{18} traverse the collimator. The beam intensity is expected to decrease from small to large angles; and should be comprised of ~ 511 keV photons at small angles, and lower energy photons at larger angles. We confirmed this expected beam structure with a NaI(Tl) detector.

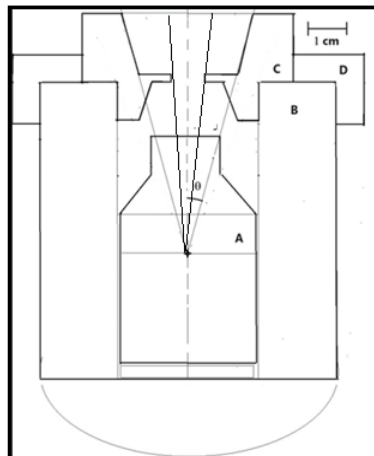


Fig.1: Scale drawing (see upper right corner) of the F^{18} source, showing A: Glass vial containing liquid FDG, B: Tungsten container, C: Tungsten Collimator, D: Fixture of the collimator to the tungsten container made of aluminum. The geometric beam angle $\theta = 16^\circ$ is shown with respect to the vial's center axis.

Beam profile

The geometry of the beam was checked by direct measurement, as shown in Fig. 2a. The source was positioned far from walls, and dose measurements were carried out 50 cm from the source, as shown in the figure. Since the detector measures dose rate, it is sensitive to the energy of detected photons, and is therefore sensitive to the angular distribution of scattered photons. Dose measurements in $\mu\text{Sv/h}$ were carried out with the Atomtex dose meter [7] over a range $x = \pm 50$ cm, as shown in the figure. Fig. 2b

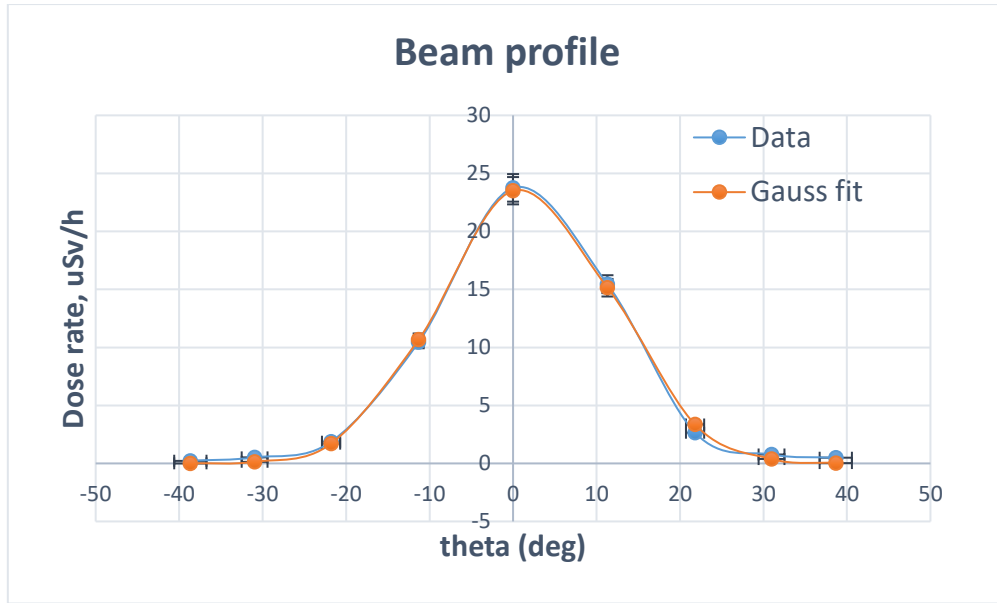


Fig. 2b: Radiation dose rate measured as a function of the angle θ relative to the beam axis, together with a chi-square fit to a Gauss function.

Atomtex AT1123 Radiation Survey Meter (Dosimeter)

This dosimeter uses a plastic scintillator (diameter 3 cm, thickness 1.5 cm) to detect a high energy photon (511 keV) by converting it into numerous low energy photons (visible light) in the range 1.6 – 3.3 eV through the process of scintillation. A single 511 keV photon interacts with an electron in the plastic scintillator via the photoelectric effect or Compton scattering. This secondary energetic electron interacts with and promotes many atoms or molecules in the scintillator to excited states. When such excited atoms quickly return to their ground states, they release energy in the form of low energy photons (visible light). The light flash intensity from all these deexciting atoms is proportional to the energy deposited by the incident high energy photon. The visible light photons release electrons from a photocathode. A photomultiplier then converts this pulse of electrons into a pulse of electric charge whose integrated charge is proportional to the incident high energy photon energy. The charge carried by this pulse provides a measure of the energy deposited in the plastic. The size and count rate measurement of these pulses determines the rate of energy deposition by a flux of high energy photons from a radiation source. The detector is calibrated using a calibrated photon source.

Measurement Method

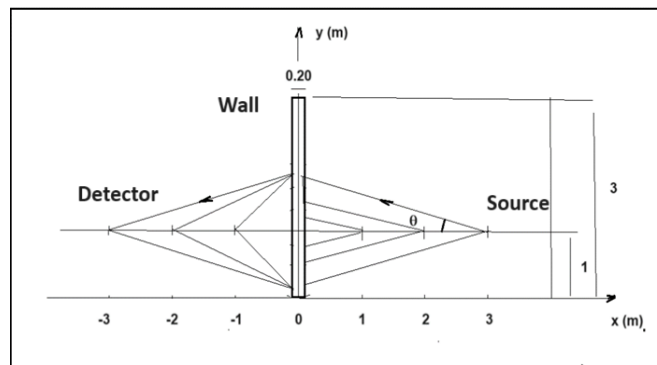


Fig. 3: Experimental Setup showing variable distance options.

All measurements were carried out with the same source. Fig. 3 shows the experimental setup. The source, positioned 3 meters from the wall, yielded a 0.64 m beam disk radius (wide-beam) on the wall. Dose rates were measured by an Atomtex AT1123 Radiation Survey Meter [7], positioned at seven distances between 0.05 to 3 meters from the far side of the wall, and eight such measurements were averaged. The measurement uncertainty was taken as the standard deviation (RMS) of the eight measurements. Distances were measured by a tape measure. The measurement setup roughly simulates radiation emitted from a patient injected with F^{18} . The background radiation level ($\sim 0.08 \mu\text{Sv/hr}$) was subtracted from each measurement. The average photon energy reaching the detector was less than 511 keV, as is the case for the average photon energy emitted from a patient. For each measurement, the clock start and stop time was recorded. The source activity was measured immediately after each transmission measurement, and its value during a measurements was evaluated using the standard time dependent 1.8 hour half-life exponential decay factor.

The wall transmission coefficient for a given source-dosimeter distance d was calculated as $T = (\text{DR})_m / (\text{DR})_e$, where $(\text{DR})_m$ is the measured dose rate behind the wall, and $(\text{DR})_e$ is the expected dose rate with the wall removed. $(\text{DR})_e$ is calculated as [2,3,5]:

$$(\text{DR})_e = \epsilon * G * A / d^2 \quad (3)$$

Here, the source efficiency is ϵ , the source-detector distance is d , A is the average source activity during the measurement, and G is the F^{18} G-Factor [8]. The source efficiency was measured far from the wall in horizontal position, with source-dosimeter distances $d = 0.5, 1, 2, 3$ m. The efficiency, taken as the average ratio between measured and expected DRs, is $\epsilon = 0.345 \pm 0.032$. This relatively low efficiency is due to the source design, as described previously. The Atomtex AT1123 dosimeter was calibrated in a certified lab by comparison to a calibrated NIST traceable high pressure ionization chamber.

3 Theory

Stankovic et al. reported a 7.0% transmission factor for 20 cm thick concrete having density 2.30 g/cm^3 via a MC simulation of 511 keV photons centered on an ordinary concrete cylinder of diameter 1 meter; corresponding to a $B=3.2$ buildup factor. Madsen et. al. [5] reported a transmission factor of 9.0% for 20 cm thick concrete having density 2.35 g/cm^3 at 500 keV for an infinite broad beam geometry; corresponding to a $B=4.5$ buildup factor. Although MC uncertainties were not quoted, we assume them to be of order 15%.

4 Results and Discussion

We measured the transmission coefficient through an Israeli B30 concrete [9] wall (3 meter high, 20 cm thick) having density 2.30 g/cm^3 as $T = 8.6 \pm 1.8\%$, corresponding to a $B=4.0$ buildup factor. This is in good agreement with Stankovic et al. ($T=7.0 \pm 1.1\%$), and Madsen et al. ($T=9.0 \pm 1.4\%$), considering the uncertainties, and considering also the differences between our experimental setup and their MC simulations. Results are shown in Table 1. The values shown in the table are appropriate only for the particular 20 cm thickness used. All transmitted radiation doses to employees were lower than the allowed radiation dose of $10 \mu\text{Sv}$ per year [10]. The narrow-beam transmission coefficient was measured when the source was positioned 0.05 m from the wall, and the detector was positioned at seven distances between 0.05-3 m on the opposite side of the wall. We obtain $T=3.0 \pm 0.9\%$ by averaging the seven measurements; and taking the uncertainty to be the RMS deviation. Considering uncertainties, this result is consistent with the $T=2.0\%$ narrow beam calculated value.

Reference	Transmission Coefficient T	Buildup Factor B	Concrete Density ρ
Stankovic et al.	0.070 *	3.2	2.30
Present	0.086 ± 0.018	4.0 ± 0.8	2.30
Madsen et al.	0.0904 *	4.5	2.35
Narrow Data	0.030 ± 0.009	1.4 ± 0.4	2.30
Narrow Calc.	0.020 *	1.0	2.30

Table 1: Transmission Coefficients T for Ordinary Concrete. The Stankovic et al. and Madsen et al. results are via MC simulations, while the Present results are from this experiment. The values labelled by * are assumed to have uncertainties of order 15%. The Narrow Beam Data T value has a 30% uncertainty.

Note that shielding designs based exclusively on thick concrete walls, besides being space inefficient, may create construction constraints due to their weight. In addition, since ordinary concrete such as Portland has an effective atomic number around $Z=10$, 511 keV photons interact almost exclusively by one or more Compton scatterings. Transmission through such a shielding wall can be high due to a large B-factor for a very wide beam (equivalent to a moving radioactive patient) and a thick concrete wall (20 cm or even thicker). By contrast, since $Z=82$ for Lead, scattering in a Lead wall will be mainly by the photoelectric effect, which has very high cross section in Lead, so that transmission through such a wall would be very low ($<0.5\%$) for a 33 mm Lead wall thickness. Therefore, Lead is much preferred, and such Lead sheets could be held in place by mounting them on a 5 cm thick gypsum wall. Thereby, the attenuation would be achieved mainly by the Lead, while the gypsum serves for physical support.

Our objective in this study was not to design an optimum shielding wall, but rather to check by experiment the results of two available MC simulations for a 20 cm thick concrete wall. These simulations and our experiment were based on wide beam assumptions, and we found good agreement. For yet wider beam assumptions, the transmission coefficient through concrete would increase even more, and such configurations merit further study.

5 Conclusions

This study determined the protective concrete shielding thickness requirements in concrete walls of positron emission tomography (PET) and computed tomography (CT) facilities. Consider the most commonly used PET radiotracer, the radioisotope F^{18} , which emits two back-to-back 511 keV gamma rays (photons). Shielding is required to protect hospital staff during the entire time that a patient remains in the hospital. Photon transmission measurements were carried out through an Israeli B30 strength concrete wall (3 meters high, 20 cm thick) using photons emitted from an F^{18} source into a cone having a 24° FWHM dose effective aperture angle. The beam photons predominantly have 511 keV energy; but include 170-511 keV photons. The source, when positioned at 3 meters maximum distance from the wall, yielded a 0.64 m maximum beam disk radius. All measurements were carried out with the same source. The background radiation level ($\sim 0.08 \mu\text{Sv/hr}$) was subtracted from each measurement. Dose rates were measured by an Atomtex AT1123 Radiation Survey Meter, positioned at distances 0.05 to 3 meters from the far side of the wall. Our measurement setup simulates radiation emitted from a patient injected with F^{18} . For a wide-beam, thick-shielding setup, there is a “buildup” effect, as photons having reduced energies may reach the detector from Compton scattering in the wall. The buildup factor B accounts for the increase of observed radiation transmission through shielding material due to scattered radiation. We measured a narrow-beam transmission coefficient $T=3.0 \pm 0.9\%$, consistent with the theoretical value 2% calculated from NIST photon attenuation data without buildup. Madsen et. al. [5] reported a transmission factor of 9.0% for 20 cm thick concrete having density 2.35 g/cm^3 at 500 keV for an infinite broad beam geometry; corresponding to a 4.5 buildup factor. Stankovic et al. [3] reported a 7.0% transmission factor for 20 cm thick concrete having density 2.30 g/cm^3 via a MC simulation of 511 keV photons centered on an ordinary concrete cylinder of diameter 1 meter; corresponding to a 3.2 buildup factor. We measured a wide-beam

transmission coefficient of $8.6 \pm 1.8\%$; corresponding to a 4.0 buildup factor; in good agreement with these two wide-beam Monte Carlo (MC) simulations. We confirm by experiment, complementing MC simulations, that for the concrete component of a shielding wall, explicitly taking for example 20 cm thick concrete, about four times thicker shielding is required compared to that calculated using tabulated narrow-beam, thin-shielding transmission coefficients.

5.1 Declarations

Study Limitations: None

Acknowledgments: None

Funding Source: Department of Nuclear Medicine, Sheba Medical Center, Ramat Gan, Israel

Competing Interests: None

Warning for Hazard: The liquid FDG F18 source is radioactive.

References

- [1] Nuclear Medicine, Sheba Medical Center, <https://eng.sheba.co.il/Nuclear-Medicine>
- [2] D. S. Smith, M. G. Stabin, "Exposure rate constants and lead shielding values for over 1,100 radionuclides", *Health physics*, 102(3), pp. 271-291, 2012, <https://doi.org/10.1097/HP.0b013e318235153a>
- [3] S. J. Stanković, R. D. Ilić, K. Janković, D. Bojović, B. Lončar, "Gamma Radiation Absorption Characteristics of Concrete with Components of Different Type Materials", *Acta Physica Polonica A*, 117(5), pp. 812–816, 2010, <https://doi.org/10.12693/APhysPolA.117.812>
- [4] J. H. Hubbell, S. M. Seltzer, "X-ray mass attenuation coefficients", 2004, <https://dx.doi.org/10.18434/T4D01F>
- [5] M. T. Madsen, J. R. Halama, J. Kleck, D. J. Simpkin, J. R. Votaw, R. E. Wendt III, L. E. Williams, M. V. Yester, G. Mawko, "PET and PET/CT shielding requirements", *Medical physics*, 33(1), pp. 4-15, 2006, <https://doi.org/10.1118/1.2135911>
- [6] R. A. Powsner, M. R. Palmer, E. R. Powsner, *Essentials of nuclear medicine physics and instrumentation*, 2013, Chichester, UK: Wiley-Blackwell
- [7] Atomtex AT1123 Radiation Survey Meter, <https://atomtex.com/en/at1121-at1123-x-ray-and-gamma-radiation-dosimeters>
<https://atomtex.com/sites/default/files/datasheets/at11211123.pdf>
- [8] K. Eckerman, A. Endo, "International Commission on Radiological Protection, ICRP Publication 107, Nuclear decay data for dosimetric calculations", *Ann. ICRP* 38(3), pp. 7-96, 2008, <https://doi.org/10.1016/j.icrp.2008.10.004>
- [9] A. Bentur, "Israeli Standard for aggregates, IS3, Israel Standards Institute", 2018, <https://www.gov.il/BlobFolder/reports/aggregates/he/03%20Bentur-%20Israeli%20Standard%20for%20Aggregates%20%E2%80%93IS3.pdf>
- [10] "Radiation Protection and Safety of Radiation Sources: International Basic Safety Standards, General Safety Requirements Part 3, GSR-3 IAEA", 2014, https://www-pub.iaea.org/mtcd/publications/pdf/pub1578_web-57265295.pdf